# Ultrafast Optical Switching from an Ionic to a Neutral State in Tetrathiafulvalene-p-Chloranil (TTF-CA) Observed in Femtosecond Reflection Spectroscopy

S. Iwai,[1] S. Tanaka,[2] K. Fujinuma,[2] H. Kishida,[2] H. Okamoto,[1,2,3] and Y. Tokura[1,4,5]

[1]*Correlated Electron Research Center (CERC), National Institute of Advanced Industrial Science and Technology (AIST), Tsukuba 305-0046, Japan*

[2]*Department of Advanced Materials Science, University of Tokyo, Tokyo 113-0033, Japan*

[3]*Structure and Transformation Group, PRESTO, Tokyo 113-0033, Japan*

[4]*Joint Research Center for Atom Technology (JRCAT), Tsukuba 305-0046, Japan*

[5]*Department of Applied Physics, University of Tokyo, Tokyo 113-8656, Japan*

(Received 6 August 2001; published 16 January 2002)

Ultrafast optical switching from an ionic ($I$) to a neutral ($N$) state in TTF-CA was observed in femtosecond reflection spectroscopy. Charge transfer excitation in the $I$ phase produces $N$ donor ($D^0$) acceptor ($A^0$) strings within 2 ps. These initial $N$ states decay with a lifetime of 300 ps at 4 K, but rather multiply leading to macroscopic $I$-$N$ conversion within 20 ps at 77 K just below the $N$-$I$ transition temperature $T_{NI}$. Near $T_{NI}$, we also found the evidence for the coherent motion of the macroscopic $N$-$I$ domain boundary with a period of 85 ps.

DOI: 10.1103/PhysRevLett.88.057402 PACS numbers: 78.47.+p, 73.20.Mf, 78.55.Kz

Low-dimensional electronic materials sometimes show phase transitions driven by the electron-electron and electron(spin)-lattice interactions. Recently, attempts to control those phase transitions and related macroscopic properties by optical excitations have been attracting much attention [1]. Such a phenomenon is called photoinduced phase transition (PIPT). In several low-dimensional materials, such as $\pi$-conjugated polymers [2], charge-transfer complexes [3], and transition-metal compounds [4–7], PIPTs were found to be caused in the materials locating near the electronic/structural phase boundary. On the PIPTs of these materials, it has been suggested that cooperative interactions of photoexcited states, initially produced, would play an important role. It is a new problem of solid-state physics to clarify the mechanism of PIPTs including such cooperative interactions. In addition to the academic interests, the exploration of PIPT on an ultrafast time scale is indispensable for new applications of optical switching materials.

The material we focus on in this Letter is a mixed-stack charge-transfer (CT) complex, tetrathiafulvalene-p-chloranil (TTF-CA), which is one of the typical examples showing PIPT. By lowering temperature, it undergoes a neutral ($N$) to ionic ($I$) phase transition at $T_{NI} = 81$ K, which is caused by the energy gain of the long range Coulomb attractive interaction overcoming the effective ionization energy of TTF donor ($D$) and CA acceptor ($A$) pairs [8]. The degree of CT ($\rho$) between TTF and CA changes abruptly from 0.3 to 0.7 at $T_{NI}$ [9]. In the ionic phase, each molecule has spin $S = 1/2$ constituting the 1D spin chains, which are dimerized due to the spin-Peierls mechanism. The recent x-ray and neutron studies have revealed that the dimeric molecular displacements are three-dimensionally ordered and, hence, that the ferroelectric ground state is stabilized [10,11].

Koshihara *et al.* previously reported that TTF-CA undergoes the photoinduced $N$-$I$ and $I$-$N$ transitions in several hundred ps after the photoirradiations [3]. In the studies, they used the excitation lights of 1.5–2.5 eV for $\mathbf{E} \perp \mathbf{a}$ ($\mathbf{a}$: $DA$ stacking axis), which produce the local intramolecular excitations of TTF. Their energies are much higher than that of the lowest CT transition peak (0.65 eV), and the PIPT in this case is supposed to occur after the intramolecular relaxation process. Thus, the early dynamics of the PIPT remains unraveled up to the present. More lately, Suzuki *et al.* reported the $I$-$N$ transition induced by the irradiation of lights with 1.2 eV for $\mathbf{E} \parallel \mathbf{a}$, which creates CT excitations with a large excess energy (off-resonant condition) [12]. The time characteristics of the optical response have not been obtained in PIPT triggered by neither the resonant nor off-resonant CT excitations.

In this Letter, we report the first observation of ultrafast photoinduced $I$-$N$ transition using a femtosecond pump-probe reflection spectroscopy. We focus on transition behaviors under a resonant excitation to the CT transition, which corresponds to an excitation of a neutral $DA$ pair in the ionic $DA$ stacks such as $[\ldots D^+A^-D^+A^-D^+A^- \ldots] \rightarrow [\ldots D^+A^-D^0A^0D^+A^- \ldots]$. In this condition, we have detected dynamical transition processes from the $D^0A^0$ pairs initially photogenerated to a macroscopic $N$ domain; as a first process, a $D^0A^0$ pair is converted to a 1D $N$ state that is composed of a $D^0A^0$ string. After that, 1D $N$ states make the neighboring $I$ states unstable through a cooperative interaction, and this then leads to a macroscopic $I$-$N$ transition. Moreover, we will report that the macroscopic photoinduced $I$-$N$ transition is followed by the coherent oscillation of the $NI$ domain boundary.

Single crystals of TTF-CA ($1 \times 0.5 \times 0.5$ mm$^3$ in size) were grown by the cosublimation of the component powder materials. Two optical parametric amplifiers (light-conversion TOPAS) pumped by the Ti:$Al_2O_3$ regenerative amplifier system (Spectra Physics Hurricane) operating at 1 kHz were employed as the light source in the reflection detected pump-probe measurements.

In Fig. 1(a), we present polarized reflectivity spectra of TTF-CA. The peak structure around 0.65 eV in both $I$ and $N$ phases is due to the CT transition. The structure around 2–2.5 eV indicated by the solid arrow is attributable to the intramolecular transition of TTF, whose position sensitively depends on $\rho$; its peak energy is 2.25 eV in the $I$ phase with $\rho = 0.7$ and 2.4 eV in the $N$ phase with $\rho = 0.3$ [8,9]. By measuring a reflectivity change of this band upon photoexcitation, the photoinduced $I$-$N$ conversion can be detected [3]. Figure 1(b) shows the transient change of reflectivity ($\Delta R/R$) at 4 K with a resonant excitation of the CT band (0.65 eV) for $\mathbf{E} \parallel \mathbf{a}$. Excitation density (photon number per unit area, $N_{\mathrm{ex}}$) is $1.2 \times 10^{16}\ \mathrm{cm}^{-2}$. The $\Delta R/R$ spectra are quite similar to the differential spectrum $[= (R_N - R_I)/R_I]$ shown by the broken line in the same panel, which is calculated from the reflectivity in the $I$ phase at 4 K ($R_I$) and the $N$ phase at 90 K ($R_N$). It indicates that the $N$ states are photogenerated in $I$ stacks. The spectral shape of $\Delta R/R$ is independent of excitation density in the range of $0.01–1.2 \times 10^{16}\ \mathrm{cm}^{-2}$ and also of delay time $\tau_d$ up to 500 ps.

To discuss the dynamics of the photogenerated $N$ state, we present the time evolutions of $-\Delta R/R$ at 4 K and 77 K in Figs. 2(a) and 2(b), respectively. The probe energy is set to the peak energy (2.25 eV) of the intramolecular transition of TTF in the $I$ phase. The $-\Delta R/R$ signals are accompanied by the prominent oscillations with the periods of several tenths ps. The origin of these oscillations will be discussed later. The initial responses are presented in the right panels. For the lower excitation density ($N_{\mathrm{ex}} = 0.02 \times 10^{16}\ \mathrm{cm}^{-2}$), the initial rise of the signal is detected within 500 fs that is followed by an immediate drop in the time region up to 2 ps. Then, the signal decays with the decay time of about 300 ps. For the higher excitation density ($N_{\mathrm{ex}} = 1.2 \times 10^{16}\ \mathrm{cm}^{-2}$), we also observe the fast initial rise that is, by contrast, followed by the increase of the signal. Such an increase saturates at about 20 ps but the signal does not decay at least up to 500 ps. At 77 K just below $T_{NI}$, on the other hand, the time evolutions of the signals are rather independent of the excitation density, as seen in Fig. 2(b), and are characterized by the fast rise within 500 fs and the subsequent increase to about 20 ps. Even for the lowest excitation density ($N_{\mathrm{ex}} = 0.01 \times 10^{16}\ \mathrm{cm}^{-2}$), the signal does not decay; that is in contrast with the rapid decay with the lifetime of 300 ps at 4 K.

To clarify the excitation density dependence in the dynamics of the photoinduced $N$ states, we plotted in Fig. 3(a) $-\Delta R/R$ at $\tau_d = 2$ and 500 ps as a function of $N_{\mathrm{ex}}$. The $-\Delta R/R$ values at $\tau_d = 2$ ps show the amount of the $D^0A^0$ pairs generated just after the photoirradiation. When $N_{\mathrm{ex}}$ is less than $0.15 \times 10^{16}\ \mathrm{cm}^{-2}$, the amount of the $D^0A^0$ pairs generated at the initial rise is proportional to $N_{\mathrm{ex}}$ at 4 K, as indicated by the broken line in Fig. 3(a). In this region, the signal almost disappears at $\tau_d = 500$ ps, reflecting the decay of the $N$ states with the lifetime of 300 ps. When $N_{\mathrm{ex}}$ exceeds $0.2 \times 10^{16}\ \mathrm{cm}^{-2}$, the signal at $\tau_d = 500$ ps shows a large intensity as a result of the multiplication of the $N$ states within 20 ps. At 77 K, the initial rise also shows the linear dependence on $N_{\mathrm{ex}}$ (the dash-dotted line) for small $N_{\mathrm{ex}}$ less than $0.05 \times 10^{16}\ \mathrm{cm}^{-2}$, and then saturates for the larger $N_{\mathrm{ex}}$. The $N$ states produced just after the photoirradiation at 2 ps never show a rapid decay in the sub-ns region but always multiply.

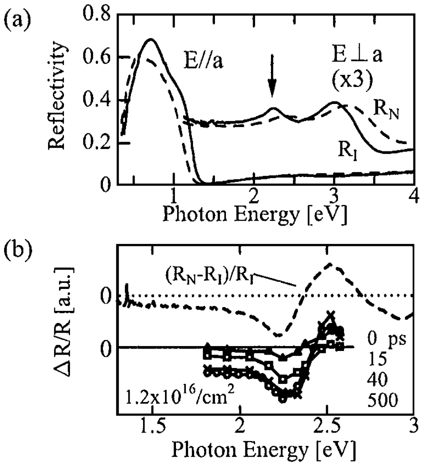

FIG. 1. (a) Polarized reflectivity spectra for $\mathbf{E} \parallel \mathbf{a}$ and $\mathbf{E} \perp \mathbf{a}$ of TTF-CA crystal on a (100) surface at 4 K (solid lines: $R_I$) and at 90 K (broken lines: $R_N$). (b) Transient differential reflection spectra ($\Delta R/R$).

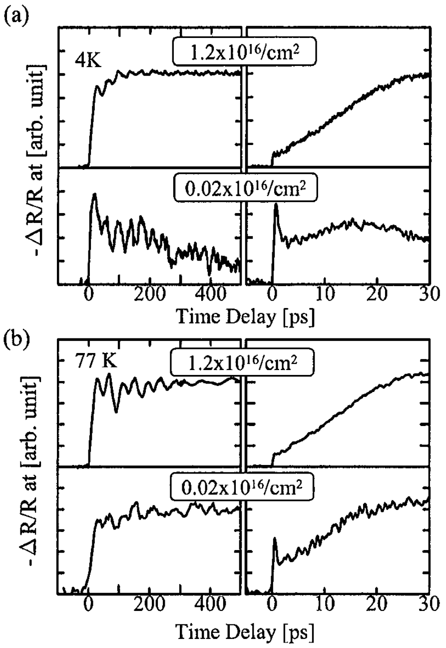

FIG. 2. Time evolutions of the transient reflectivity changes at 2.25 eV [(a) 4 K; (b) 77 K].

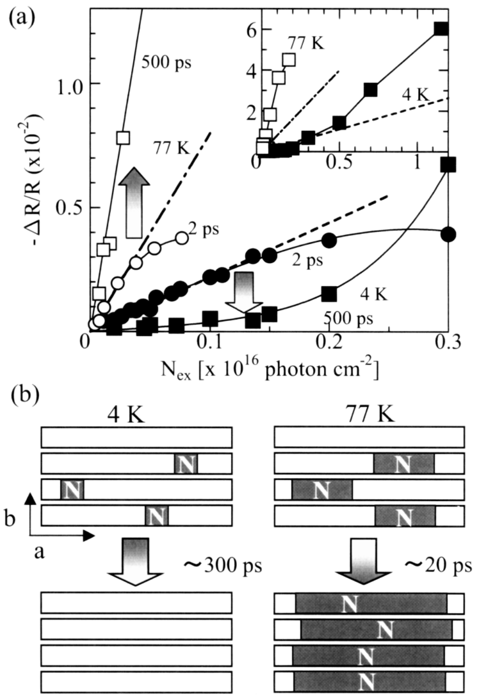

FIG. 3. (a) The $\mathbf{E}\perp\mathbf{a}$ photomodulation ($-\Delta R/R$) observed at 2.25 eV as a function of excitation density $N_{\mathrm{ex}}$; closed circles: 4 K, 2 ps; closed square: 4 K, 500 ps; open circles: 77 K, 2 ps; open squares: 77 K, 500 ps. (b) Schematic illustration of the photoinduced *I*-*N* conversion for the low excitation density.

The saturated value of $-\Delta R/R$ at $\tau_d = 2$ ps is equal to 0.004, which is nearly identical at 4 and 77 K; therefore, it is reasonable to consider that this saturation is related with the space filling of the *N* states in the *I* stacks. To estimate the amount of initial $D^0A^0$ pairs, we assume that the saturation occurs when half of the molecules within the absorption depth $L$ for the pump lights are neutralized. The amount of the $D^0A^0$ pairs will not exceed that of the $D^+A^-$ pairs, since the two CT processes, $D^+A^- \rightarrow D^0A^0$ and $D^0A^0 \rightarrow D^+A^-$, compete with each other, both of which are resonantly excited by the 0.65 eV pump. Using the saturation densities ($N_s = 0.2 \times 10^{16}$ cm$^{-2}$ at 4.2 K and $0.07 \times 10^{16}$ cm$^{-2}$ at 77 K) and $L \approx 400$ Å deduced from the analysis of the polarized reflectivity spectrum, we can estimate the amount of initial $D^0A^0$ pairs produced by one photon (a single CT excitation) to be $8D^0A^0$ at 4 K and $24D^0A^0$ at 77 K. These initial *N* states are considered to be 1D confined *N* domains relaxed from the Franc-Condon–type CT excited state. This relaxation process is schematically shown as $[\ldots D^+A^-D^+A^-D^+A^-D^0A^0D^+A^-D^+A^- \ldots] \rightarrow [\ldots D^+A^-D^0A^0D^0A^0 \ldots D^0A^0D^0A^0D^+A^- \ldots]$. It has been theoretically suggested that the energy of a 1D *N* domain is lower than that of a single CT state, when *N* and *I* phases are almost degenerate [13,14]. The evaluated size of the initial 1D *N* domain at 77 K is larger than that at 4 K. This is perhaps because the valence instability is enhanced near $T_c$. A large size of the 1D *N* domain can be regarded as an excitation of an *NI* domain wall (*DW*) pair [13]. In the time evolution of $-\Delta R/R$ shown in Fig. 2(a), the spikelike rise and decay is observed within 2 ps for the small excitation density, which might be related to the relaxation dynamics from the single CT state to the *NIDW* pair.

The *N* states produced after the multiplication have a lifetime much longer than 500 ps, suggesting the formation of stable states, which are distinct from the 1D *N* domains initially produced. It is reasonable to consider that the 1D *N* domains make the neighboring *I* states unstable and change them to *N* states, resulting in the production of macroscopic *N* regions. The *I* phase in TTF-CA is stabilized by the interchain interactions as well as the intrachain one, as demonstrated by the detailed structural analysis [11]. As for the interchain interaction, there are two kinds of energy gain stabilizing the macroscopic *I* phase; one is due to the interchain Coulomb interaction, and the other to the 3D ordering of dimeric displacements giving rise to the ferroelectric nature. Both energy gains will be lost by the generation of the 1D *N* domains. That would be the reason why the multiplication of the 1D *N* domains to the macroscopic *N* region occurs. At 77 K, the multiplication occurs even for a very low excitation density of $0.005 \times 10^{16}$ cm$^{-2}$, which corresponds to 1 photon/340 *DA* pairs. Such an enhanced multiplication of the *N* states at 77 K is again attributable to increasing the valence instability near $T_{NI}$. The observed photoinduced *I*-*N* conversion for the low excitation density is illustrated in Fig. 3(b).

Now, let us proceed to the discussion about the oscillation in the time evolution of $-\Delta R/R$. To analyze these oscillations, we subtracted the exponential rise and decay from the time profile at 77 K with $N_{\mathrm{ex}} = 1.2 \times 10^{16}$ cm$^{-2}$. Figure 4(a) shows the residual oscillating components, which are composed of two oscillations having different periods. We have tried to fit the data with a superposition of two exponentially damped oscillations, $\sum_{i=1}^{2} A_i \cos(\omega_i t - \phi_i) \exp(-t/\tau_i)$. The thin solid lines are the calculated results, which well reproduce the experimental ones.

Figure 4(b) shows the quantum energy of the oscillation ($\Delta E = \hbar\omega$) as a function of twice the wave number of probe light $k(= 2\pi n/\lambda)$ in the sample. In Fig. 4(c), the amplitude of the oscillations is displayed as a function of the probe energy. In the lower frequency oscillations, the phase ($\phi$) is almost constant for the probe energies of 1.77–2.25 eV, but shifts relatively by $\pi$ at 2.53 eV. Such a shift of $\phi$ is interpreted as a change of the sign of the amplitude in Fig. 4(c). In the higher frequency oscillations, on the other hand, $\phi$ is independent of the probe energy.

The amplitude of the higher frequency oscillation is almost constant irrespective of the probe energy. However, its $\Delta E$ rather depends on the probe energy being proportional to $2k$. From these features, this oscillation is attributable to the shock wave, which is generated via the photoinduced impulsive mechanical stress. In the temperature induced *NI* transition, the unit cell volume decreases

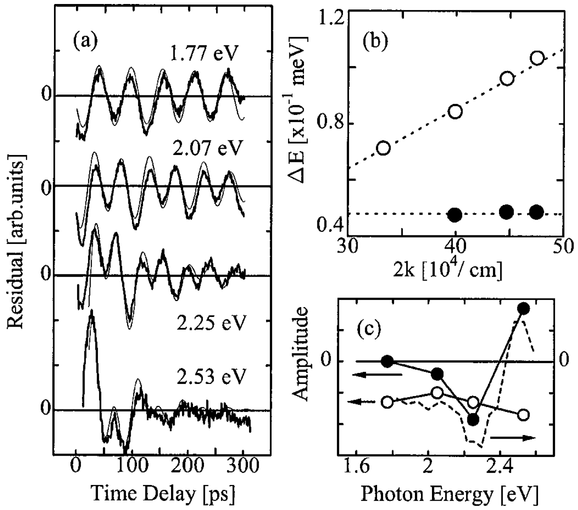

FIG. 4. (a) Oscillatory components observed at 77 K with $N_{\mathrm{ex}} = 1.2 \times 10^{16}$ cm$^{-2}$. (b) Quantum energy of the oscillation ($\Delta E = \hbar\omega$) as a function of $2k$ of the probe photon (closed circles: low frequency; open circles: high frequency). (c) Amplitudes of high-frequency (open circles) and low-frequency (closed circles) oscillations at each probe photon energy. Spectrum of the $\Delta R/R$ observed at 500 ps after excitation is superimposed by the broken curve.

by 0.6% across $T_{NI}$ [10]. Therefore, photoinduced *IN* conversion will produce a sudden volume change, which acts as a broadband source of acoustic phonons. In this case, the monochromatic probe light should be modulated by the phonon having the wave number $2k$. A relation between the modulation frequency and $2k$ corresponds to a dispersion of the acoustic phonon. The observed linear relation between $\Delta E$ and $2k$ demonstrates this interpretation. The sound velocity is evaluated as $0.65 \times 10^5$ cm/s. This kind of oscillation in photoinduced reflectivity change has been previously reported in the photoinduced melting of a charge-ordered state of perovskite manganite [15].

As for the lower frequency oscillation, $\Delta E$ does not depend on the probe energy, and the amplitude profile is in good agreement with that of $-\Delta R/R$ shown by the broken line in Fig. 4(c). Therefore, this oscillation is related to the change of the molecular ionicity. There are two possibilities as the origin of this oscillation. One is a modulation in the degree of CT $\rho$. It should couple with the optical phonon corresponding to the dimeric molecular displacements, the frequency of which is ca. 30 cm$^{-1}$ (1 ps) [16]. This is, however, much larger than the observed frequency 0.4 cm$^{-1}$ (85 ps). Another possible origin is a modulation in the amount of the *N* states. To pursue this possibility, we measured temperature dependence of the oscillation. Figure 5(a) shows the power spectra obtained from the time profiles of $-\Delta R/R$ at 2.25 eV by using the Fourier transformation. As shown in Fig. 5(b), intensity of the lower-frequency band ($I_l$) relative to the higher-frequency band ($I_h$) is considerably enhanced with the increase of temperature up to $T_{NI}$. Therefore, the lower-frequency oscillation can be attributed to the modulation in the amount of the *N* state. It is to be noted that this oscillation starts at $\tau_d \approx 20$ ps when the multiplication of the 1D *N* states to the macroscopic *N* domain is almost completed. It indicates that this oscillation is not relevant to the microscopic 1D *N* domains, but to the modulation in the size of the macroscopic *N* domain, or, equivalently, the coherent motion of the *NI* domain boundary over a macroscopic scale.

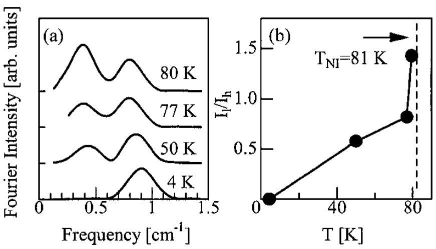

FIG. 5. (a) Fourier power spectra of the oscillatory components observed at various temperatures. (b) The ratio between the amplitudes of low-frequency ($I_l$) and high-frequency ($I_h$) peak.

In conclusion, we observed ultrafast *I-N* transition of TTF-CA by the resonant CT excitation. The microscopic 1D *N* domains are initially produced within 2 ps. At 4 K, they decay rapidly with a lifetime of 300 ps for the low excitation density, but rather multiply within 20 ps for the high excitation density through a cooperative interstack interaction. At 77 K, the enhancement of the valence instability promotes the multiplication of the 1D *N* domains, and the macroscopic *I-N* transition occurs even for very low excitation density. In addition, we found the coherent motion of the macroscopic *N-I* domain boundary for the first time.

[1] *Relaxations of Excited States and Photoinduced Structural Phase Transitions,* edited by K. Nasu, Springer Series in Solid State Science Vol. 124 (Springer-Verlag, Berlin, 1997).
[2] S. Koshihara *et al.,* Phys. Rev. Lett. **68**, 1148 (1992).
[3] S. Koshihara *et al.,* Phys. Rev. B **42**, 6853 (1990); S. Koshihara *et al.,* J. Phys. Chem. B **103**, 2592 (1999).
[4] A. Hauser, J. Chem. Phys. **94**, 2741 (1994).
[5] O. Sato *et al.,* Science **272**, 704 (1996).
[6] M. Fiebig *et al.,* Science **280**, 1925 (1998).
[7] Y. Ogawa *et al.,* Phys. Rev. Lett. **84**, 3181 (2000).
[8] J. B. Torrance *et al.,* Phys. Rev. Lett. **47**, 1747 (1981).
[9] Y. Tokura *et al.,* Solid State Commun. **43**, 757 (1982).
[10] M. Le Cointe *et al.,* Phys. Rev. B **51**, 3374 (1995).
[11] M. H. Lemee-Cailleau *et al.,* Phys. Rev. Lett. **79**, 1690 (1997).
[12] T. Suzuki *et al.,* Phys. Rev. B **60**, 6191 (1999).
[13] N. Nagaosa *et al.,* J. Phys. Soc. Jpn. **55**, 2745 (1986); **55**, 3488 (1986).
[14] Y. Toyozawa, Solid State Commun. **84**, 255 (1992).
[15] M. Fiebig *et al.,* Appl. Phys. B **71**, 211 (2000).
[16] Y. Okimoto *et al.,* Phys. Rev. Lett. **87**, 187401 (2001).